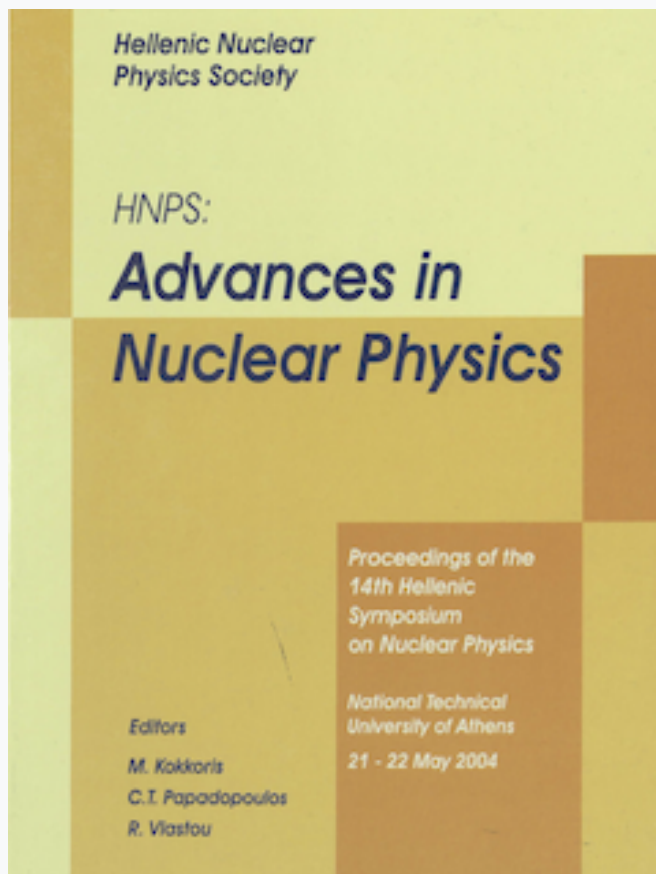


## HNPS Advances in Nuclear Physics

Vol 13 (2004)

HNPS2004



### Relativistic Hartree-Bogoliubov description of deformed light nuclei

G. A. Lalazissis, D. Vretenar, P. Ring

doi: [10.12681/hnps.2948](https://doi.org/10.12681/hnps.2948)

#### To cite this article:

Lalazissis, G. A., Vretenar, D., & Ring, P. (2020). Relativistic Hartree-Bogoliubov description of deformed light nuclei. *HNPS Advances in Nuclear Physics*, 13, 1–9. <https://doi.org/10.12681/hnps.2948>

# Relativistic Hartree-Bogoliubov description of deformed light nuclei

G. A. Lalazissis<sup>a</sup> D. Vretenar<sup>b</sup> P. Ring<sup>c</sup>

<sup>a</sup>*Department of Theoretical Physics, Aristotle University of Thessaloniki,  
Thessaloniki Gr-54124, Greece*

<sup>b</sup>*Physics Department, Faculty of Science, University of Zagreb,  
10000 Zagreb, Croatia*

<sup>c</sup>*Physik-Department der Technischen Universität München,  
D-85748 Garching, Germany*

---

## Abstract

The Relativistic Hartree-Bogoliubov model is applied in the analysis of ground-state properties of light nuclei with  $4 \leq Z \leq 11$ . The model uses the NL3 effective interaction in the mean-field Lagrangian, and describes pairing correlations by the pairing part of the finite range Gogny interaction D1S. Neutron separation energies, quadrupole deformations, nuclear matter radii, and differences in radii of proton and neutron distributions are compared with recent experimental data

*Key words:* PACS: 21.60.Jz, 21.10.Dr, 21.10.Gv, 27.20.+n, 27.30.+t

---

## 1 Introduction

The last decade a large quantity of data on light nuclei with  $4 \leq Z \leq 12$  has become available. Measurements of interaction cross sections by using radioactive nuclear beams at intermediate and relativistic energies, have provided important data on nuclear radii [1–9]. The nuclear radius is a fundamental quantity which, in principle, provides information on the effective nuclear potential, shell effects and ground-state deformation. For exotic nuclei with extreme values of neutron to proton ratio, particularly important is the isospin dependence of nuclear radii which can signal the onset of new phenomena like, for example, the formation of skin and halo structures.

The Relativistic Hartree-Bogoliubov (RHB) model has been applied recently [10] in the analysis of ground-state properties of Be, B, C, N, F, Ne and

Na isotopes. Based on the relativistic mean-field theory and on the Hartree-Fock-Bogoliubov framework, the RHB model provides a unified description of mean-field and pairing correlations. A detailed description of the model can be found in Ref. [29]. The theory has been successfully applied in the description of nuclear structure phenomena in exotic nuclei far from the valley of  $\beta$ -stability and of the physics of the drip lines (for a recent review see Ref. [11]).

In this paper results for isotopic chains of light nuclei with odd  $Z$  are reported. In section 2, the results are presented and discussed, while section 3 summarizes the main conclusions.

## 2 Ground-state properties of deformed light nuclei

In the present work we apply the RHB model, with the NL3+D1S effective interaction, in the analysis of ground state properties of B, N, F, and Na isotopic sequences. We perform deformed RHB calculations and compare radii, separation energies and quadrupole deformations with available experimental data and with the predictions of the finite range droplet model (FRDM) [42]. Of course, when the RHB equations are solved in the configuration space of harmonic oscillator basis states, for nuclei at the drip lines one does not expect an accurate description of properties that crucially depend on the spatial extension of the wave functions of the outermost nucleons, especially on the neutron-rich side. In Fig. 1 we display the proton, neutron and matter radii, ground-state quadrupole deformations, and one-neutron separation energies of Boron isotopes, calculated with the NL3 + Gogny D1S effective interaction. The calculated matter radii are in excellent agreement with the recent experimental data [6,7] for  $^{17}\text{B}$  and  $^{19}\text{B}$ , while they are larger than the older experimental values [1] for  $^{14}\text{B}$  and  $^{15}\text{B}$ . Unlike in the case of Be, the calculated proton radii for these two nuclei agree well with the empirical values, but the theoretical neutron radii are much larger. The RHB calculation also predicts  $^{14}\text{B}$  and  $^{15}\text{B}$  to be spherical in the ground state, while the heavier Boron isotopes are strongly prolate deformed. We find a sudden onset of strong deformation at  $A = 17$ . The experimentally observed Q-moments change rather smoothly from  $|Q(^{13}\text{B})| = 36.9$  mb over  $|Q(^{15}\text{B})| = 38.0$  mb to  $|Q(^{15}\text{B})| = 38.8$  mb. This can be explained as a deficiency of mean field theory, which shows always very sharp phase transitions reflecting the properties of infinite systems where fluctuations can be neglected. In such light nuclei fluctuations play an important role and therefore the experimental quadrupole moments change usually much more smoothly than those predicted by mean field calculations. The separation energies agree with the empirical values [43], and we note that both  $^{16}\text{B}$  and  $^{18}\text{B}$  are predicted to be neutron unbound.

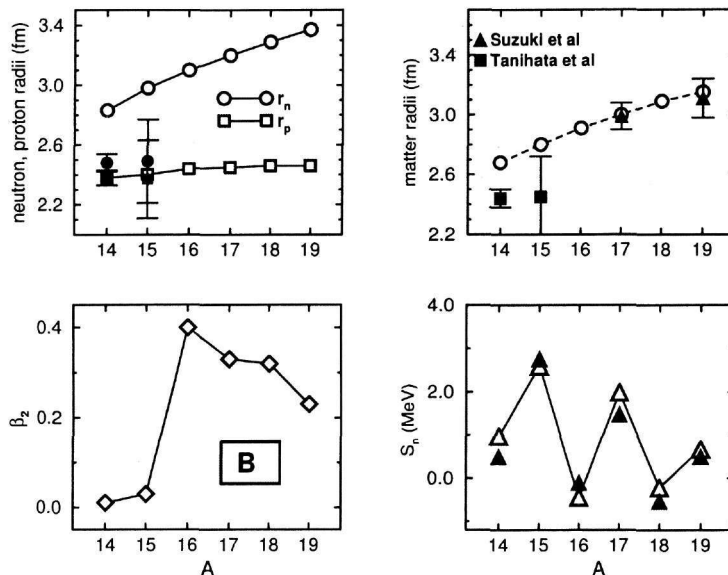


Fig. 1. Proton, neutron and matter radii, ground-state quadrupole deformations and one-neutron separation energies of Boron isotopes, calculated with the NL3 + Gogny D1S effective interaction. The theoretical values are compared with the experimental radii [1,6,8] and separation energies [43].

The RHB results for Nitrogen isotopes are shown in Fig. 2. The proton radii are compared with the experimental values from Ref. [46]. The calculated matter radii reproduce the global trend of the experimental data [8], but not the sudden increase of the radii at  $N=15$ . In the recent measurement of the interaction cross sections for  $^{14-23}\text{N}$ ,  $^{16-24}\text{O}$ , and  $^{18-26}\text{F}$  on Carbon targets at relativistic energies [8], a sharp increase of matter radii at  $N=15$  was observed in all three isotopic chains (see also Fig. 3). The deduced matter radii for  $^{22}\text{N}$ ,  $^{23}\text{O}$ , and  $^{24}\text{F}$  are much larger than those of their respective neighbors with one neutron less, and the deduced nucleon density distributions show a long neutron tail for these nuclei, comparable to that in  $^{11}\text{Be}$ . It was therefore concluded that these three nuclei exhibit a one-neutron halo structure. Since they are spherical, the halo structure should result from the odd neutron occupying the  $2s_{1/2}$  orbital. The absence of the centrifugal barrier for an  $s$ -orbital facilitates the formation of the long tail of the wave function, i.e. the halo structure. However, in Ref. [8] it was also noted that the one-neutron separation energies for  $^{22}\text{N}$ ,  $^{23}\text{O}$ , and  $^{24}\text{F}$  are larger than 1 MeV ( $1.22 \pm 0.22$  MeV,  $2.74 \pm 0.12$  MeV and  $3.86 \pm 0.11$  MeV, respectively), and much larger than in  $^{11}\text{Be}$  and  $^{19}\text{C}$ . In a recent analysis [49] it has been pointed out that the conventional

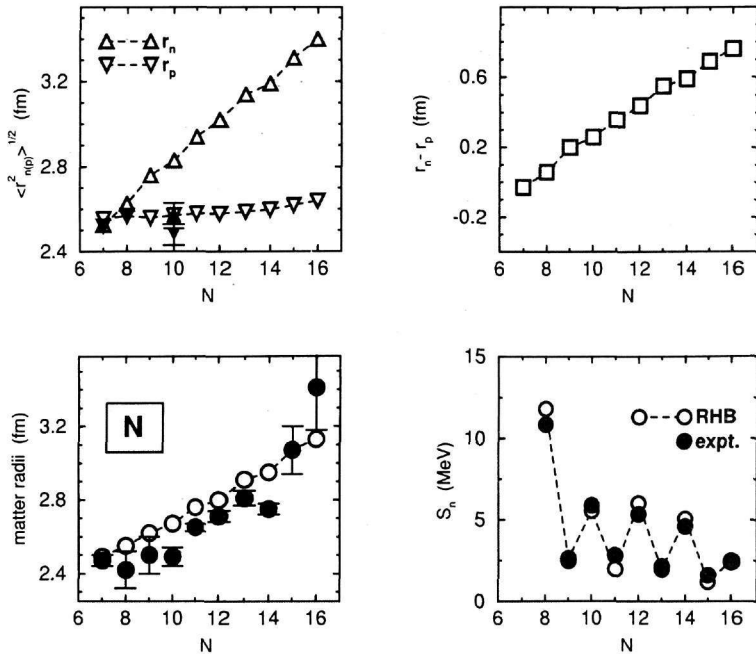


Fig. 2. The RHB theoretical proton, neutron and matter radii, skin thicknesses, and one-neutron separation energies of Nitrogen isotopes, compared with the experimental radii [46,2,8] and separation energies [43].

fixed core-plus-neutron model for halo nuclei is unable to explain the observed enhanced cross section for these nuclei with any selection of neutron orbitals, and therefore a possibility of an enlarged core structure has been suggested. Experimental evidence of core modification in the near-drip nucleus  $^{23}\text{O}$  has been recently reported in Ref. [50]. The present RHB calculation reproduces the empirical one-neutron separation energies [43]. In particular, for  $^{22}\text{N}$  we even obtain a slightly lower one-neutron separation energy, and the theoretical matter radius coincides with the one deduced from the experimental interaction cross section. Also for  $^{23}\text{N}$ , the calculated and empirical separation energies coincide, and the theoretical matter radius is only slightly below the large experimental error bar. The main difference is in the matter radii of the lighter isotopes (a similar situation also occurs for the Fluorine isotopes, see Fig. 3). The calculated radii are somewhat larger than the experimental values and therefore at  $N=15$  do not display the sharp discontinuity which, in Ref. [8], is taken as evidence for the formation of the neutron halo. In the present calculation the gradual increase of matter radii reflects the formation of the neutron skin. This is shown in the upper right panel of Fig. 2, where the values of  $r_n - r_p$  are plotted as function of the neutron number. It should be pointed out, however, that the formation of the halo structure can only be ob-

served if calculations were performed in coordinate space. Moreover, particle number projection might be necessary in order to reproduce the sharp increase of matter radii. Finally, we note that the RHB NL3+D1S calculation predicts the heaviest particle stable Nitrogen isotope to be  $^{23}\text{N}$ , in excellent agreement with recent data on the neutron drip-line [12]. Very similar results are obtained for the Fluorine isotopes. In Fig. 3 we compare the RHB theoretical proton, neutron and matter radii, and one-neutron separation energies with the experimental radii [2,8,46] and separation energies [43]. The calculated matter radii do not reproduce the discontinuity at  $N=15$ , though for the heaviest isotopes they are found within the experimental error bars. The calculated one-neutron separation energies reproduce the staggering between even- $N$  and odd- $N$  values. It is interesting to note that, like in the case of Nitrogen, the RHB model with the NL3+D1S effective interaction correctly predicts the location of the drip-line [12]: the last bound isotope of Fluorine is  $^{31}\text{F}$ . Therefore, in agreement with experimental data, we obtain that the neutron drip-line is at  $N=16$  for  $Z=7$ , and at  $N=22$  for  $Z=9$ . On the other hand, none of the standard RMF effective interactions reproduces the location of the drip-line for Oxygen. It has been argued that the sudden change in stability from Oxygen to Fluorine may indicate the onset of deformation for the neutron-rich Fluorine isotopes [12]. In the present calculation, however, all Fluorine isotopes up to  $^{31}\text{F}$  turn out to be essentially spherical. The ground-state properties of the Na isotopic sequence are illustrated in Fig. 4. The one-neutron separation energies are shown in comparison with experimental data [43]. The calculated values reproduce the empirical staggering between even- and odd- $A$  isotopes, although for  $A > 24$  the theoretical separation energies are systematically somewhat larger for the even- $N$  isotopes. The calculated radii are compared with the experimental data: matter radii [5], neutron radii [3], and charge isotope shifts [51]. An excellent agreement between theory and experiment is obtained. For the matter and neutron radii the only significant difference is at  $A=22$ , but this dip in the experimental sequence has recently been attributed to an admixture of the isomeric state in the beam [5]. Except for the lightest isotope shown, i.e.  $^{20}\text{Na}$ , the calculated charge isotope shifts reproduce the empirical  $A$ -dependence. A significant difference between the theoretical and experimental values is observed only for  $A \geq 29$ . The calculated ground-state quadrupole deformations of the Na isotopes are compared with the predictions of the finite-range droplet model [42]. We note that, while the FRDM predicts all Na isotopes with  $A \leq 28$  to be strongly prolate deformed, the result of the RHB calculation is the staggering between prolate and oblate shapes, indicating the onset of shape coexistence. In particular,  $^{26,27}\text{Na}$  are predicted to be oblate, while prolate ground-state deformations are calculated for  $^{28,29}\text{Na}$ . Very recent experimental data on quadrupole moments of  $^{26-29}\text{Na}$  [52] confirm this prediction.

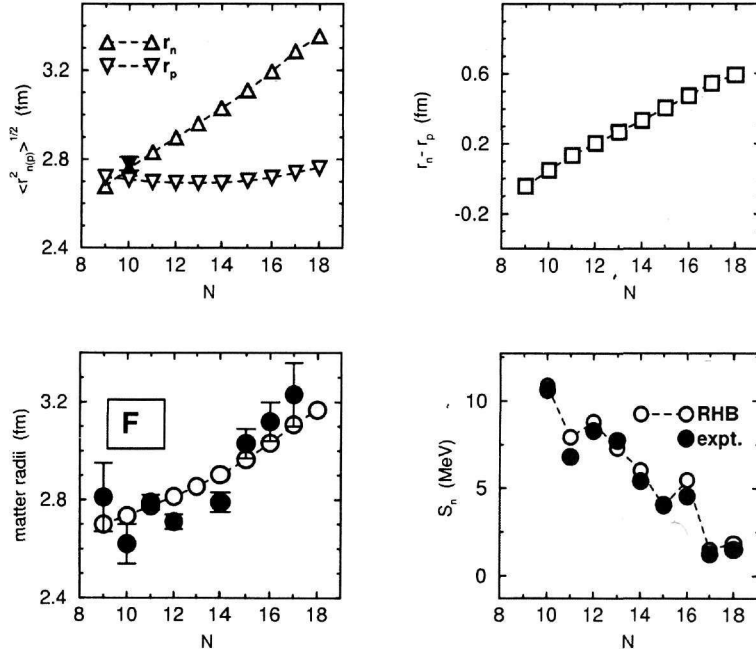


Fig. 3. The RHB theoretical proton, neutron and matter radii, skin thicknesses, and one-neutron separation energies of Fluorine isotopes, compared with the experimental radii [46,2,8] and separation energies [43].

### 3 Summary

This work presents an analysis of ground-state properties of B, N, F, Na isotopes in the framework of the Relativistic Hartree-Bogoliubov (RHB) model. The present analysis covers a region which is probably at the low-mass limit of applicability of the mean-field framework. This work is also a continuation of our previous applications of the RHB model of Ref. [20] and [31]. The present calculation has been performed in the configuration space of a deformed harmonic oscillator basis states. The NL3 effective interaction has been used for the mean-field Lagrangian, and pairing correlations have been described by the pairing part of the finite range Gogny interaction D1S. The calculated neutron separation energies, quadrupole deformations, nuclear matter radii, and differences in radii of proton and neutron distributions have been compared with very recent experimental data. For the neutron-rich Boron isotopes, the calculated matter radii reproduce the recent experimental data [6] for  $^{17}\text{B}$  and  $^{19}\text{B}$ . This is an important result, since  $^{19}\text{B}$  ( $T_z = 9/2$ ) has one of the largest  $N/Z$  values known at present in the low-mass region of the nuclear chart. The RHB model with the NL3+D1S effective interaction predicts the location of

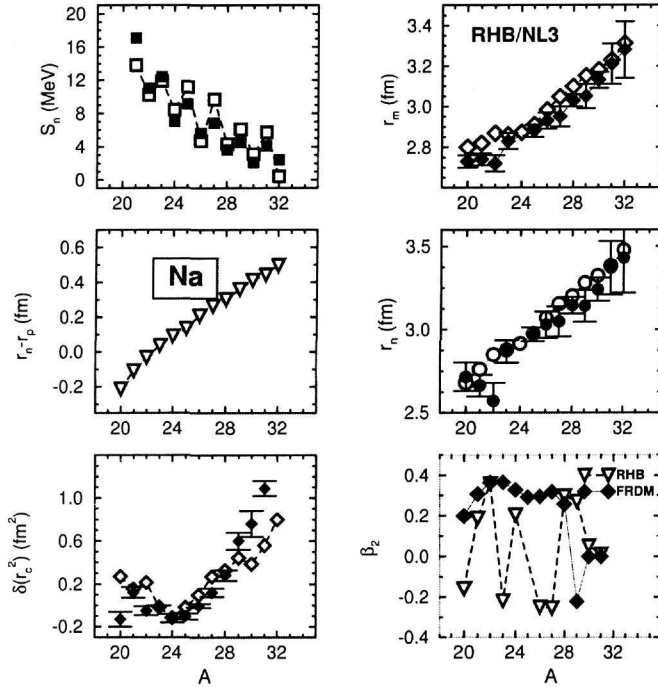


Fig. 4. One-neutron separation energies, radii, charge isotope shifts and ground-state quadrupole deformations of Sodium isotopes. The RHB calculated values are compared with the experimental data: one-neutron separation energies [43], matter radii [5], neutron radii [3], charge isotope shifts [51], and with the  $\beta_2$  values calculated in the finite-range droplet model [42].

the neutron drip-line in Nitrogen and Fluorine in agreement with recent experimental findings [12]: the heaviest particle stable isotopes are  $^{23}\text{N}$  and  $^{31}\text{F}$ . The calculated matter radii of the neutron-rich Nitrogen and Fluorine isotopes are in agreement with very recent experimental data [8]. The sudden increase of the radii at  $N=15$ , which was taken as evidence for the formation of the neutron halo, is not reproduced by the present calculation. For the Na isotopic sequence the calculated radii are in excellent agreement with experimental data on matter radii [5], neutron radii [3], and charge isotope shifts [51]. The calculated ground-state quadrupole deformations are confirmed by the recent experimental data on quadrupole moments of  $^{26-29}\text{Na}$  [52].

#### 4 Acknowledgements

This work has been supported by BMFB (06 MT 133), DFG, GSI and by the Greek Ministry of National Education and Religious affairs (Pythagoras II).

## References

- [1] I. Tanihata *et al.*, Phys. Lett. **B206**, 592 (1988).
- [2] A. Ozawa *et al.*, Phys. Lett. **B334**, 18 (1994).
- [3] T. Suzuki *et al.*, Phys. Rev. Lett. **75**, 3241 (1995).
- [4] A. Ozawa *et al.*, Nucl. Phys. **A608**, 63 (1996).
- [5] T. Suzuki *et al.*, Nucl. Phys. **A630**, 661 (1998).
- [6] T. Suzuki *et al.*, Nucl. Phys. **A658**, 313 (1999).
- [7] T. Suzuki *et al.*, Phys. Rev. Lett. **89**, 012501 (2002).
- [8] A. Ozawa *et al.*, Nucl. Phys. **A691**, 599 (2001).
- [9] A. Ozawa *et al.*, Nucl. Phys. **A693**, 32 (2001).
- [10] G. A. Lalazissis, D. Vretenar, P. Ring, Eur. Phys. J. **A22**, 37 (2004).
- [11] D. Vretenar, A. V. Afanasjev, G. A. Lalazissis, and P. Ring, Physics Reports **409**, 101 (2005).
- [12] H. Sakurai *et al.*, Phys. Lett. **B448**, 180 (1999).
- [13] P. J. Woods and C. N. Davids, Annu. Rev. Nucl. Part. Sci. **47**, 541 (1997).
- [14] Y. N. Novikov *et al.*, Nucl. Phys. **A697**, 92 (2002).
- [15] A. Leistenschneider *et al.*, Phys. Rev. Lett. **86**, 5442 (2001).
- [16] L. Chulkov, Nucl. Phys. **A603**, 219 (1996).
- [17] J. Gómez del Campo *et al.*, Phys. Rev. Lett. **86**, 43 (2001).
- [18] J. Meng and P. Ring, Phys. Rev. Lett. **77**, 3963 (1996).
- [19] W. Pöschl, D. Vretenar, G. A. Lalazissis, and P. Ring, Phys. Rev. Lett. **79**, 3841 (1997).
- [20] G. A. Lalazissis, D. Vretenar, W. Pöschl, and P. Ring, Nucl. Phys. **A632**, 363 (1998).
- [21] G. A. Lalazissis, D. Vretenar, W. Pöschl, and P. Ring, Phys. Lett. **B418**, 7 (1998).
- [22] G. A. Lalazissis, D. Vretenar, P. Ring, M. Stoitsov, and L. Robledo, Phys. Rev. **C60**, 014310 (1999).
- [23] J. Meng and P. Ring, Phys. Rev. Lett. **80**, 460 (1998).
- [24] J. Meng, Nucl. Phys. **A654**, 702c (1999).
- [25] G. A. Lalazissis, D. Vretenar, and P. Ring, Phys. Rev. **C57**, 2294 (1998).

- [26] J. Meng, Nucl. Phys. **A635**, 3 (1998).
- [27] J. Meng and I. Tanihata, Nucl. Phys. **A650**, 176 (1999).
- [28] D. Vretenar, G. A. Lalazissis, and P. Ring, Phys. Rev. Lett. **82**, 4595 (1999).
- [29] G. A. Lalazissis, D. Vretenar, and P. Ring, Nucl. Phys. **A650**, 133 (1999).
- [30] G. A. Lalazissis, D. Vretenar, and P. Ring, Nucl. Phys. **A679**, 481 (2001).
- [31] G. A. Lalazissis, D. Vretenar, and P. Ring, Phys. Rev. **C63**, 034305 (2001).
- [32] P. Ring, Progr. Part. Nucl. Phys. **37**, 193 (1996).
- [33] J. Boguta and A. R. Bodmer, Nucl. Phys. **A292**, 413 (1977).
- [34] W. Pöschl, D. Vretenar, and P. Ring, Comput. Phys. Commun. **103**, 217 (1997).
- [35] Y. K. Gambhir, P. Ring, and A. Thimet, Ann. Phys. (N.Y.) **198**, 132 (1990).
- [36] M. Serra and P. Ring, Phys. Rev. **C65**, 064324 (2002).
- [37] G. A. Lalazissis, J. König, and P. Ring, Phys. Rev. **C55**, 540 (1997).
- [38] J. F. Berger, M. Girod, and D. Gogny, Nucl. Phys. **A428**, 32 (1984).
- [39] P.-G. Reinhard, M. Rufa, J. Maruhn, W. Greiner, and J. Friedrich, Z. Phys. **A323**, 13 (1986).
- [40] M. M. Sharma, M. A. Nagarajan, and P. Ring, Phys. Lett. **B312**, 377 (1993).
- [41] Y. Sugahara and H. Toki, Nucl. Phys. **A579**, 557 (1994).
- [42] P. Möller, J. R. Nix, W. D. Myers, and W. J. Swiatecki, At. Data Nucl. Data Tables **59**, 185 (1995).
- [43] G. Audi and A. H. Wapstra, Nucl. Phys. **A595**, 409 (1995).
- [44] M. Fukada *et al.*, Phys. Lett. **B268**, 339 (1991).
- [45] J. H. Kelley *et al.*, Phys. Rev. Lett. **74**, 30 (1995).
- [46] H. de Vries, C. W. de Jager, and C. de Vries, At. Data Nucl. Data Tables **36**, 495 (1987).
- [47] D. Bazin *et al.*, Phys. Rev. Lett. **74**, 3569 (1995).
- [48] T. Nakamura *et al.*, Phys. Rev. Lett. **83**, 1112 (1999).
- [49] R. Kanungo, I. Tanihata, and A. Ozawa, Phys. Lett. **B512**, 261 (2001).
- [50] R. Kanungo *et al.*, Phys. Rev. Lett. **88**, 142502 (2002).
- [51] E. W. Otten, in *radii isotope shifts by laser beam spectroscopy*, edited by D. A. Bromley (Plenum, New York, 1989), Vol. 8, p. 515.
- [52] M. Keim *et al.*, Eur. Phys. J. **8**, 31 (2000).